

PACS numbers: 32.80.Fb; 33.80.Eh; 07.79.–v; 42.65.Re
DOI: 10.1070/QE2013v043n04ABEH015107

Microscopy of photoionisation processes

S.A. Aseyev, B.N. Mironov, V.G. Minogin, A.P. Cherkun, S.V. Chekalin

Abstract. **A method is demonstrated which combines the ionisation of free molecules by a sharply focused femtosecond laser beam and projection microscopy in a divergent electric field. The electric field is produced in vacuum between a metallic tip and a flat position-sensitive charged particle detector. The method enables investigation of photoionisation processes in low-density gases with a subdiffraction spatial resolution and can be used as well in profile measurements for sharply focused, intense laser beams. In a demonstration experiment, a femtosecond laser beam with a peak intensity of $\sim 10^{14}$ W cm^{-2} was focused to a 40-μm-diameter waist in vacuum near a millimetre-size tip and ~2-μm spatial resolution was achieved. According to our estimates, the use of a sharper tip will ensure a submicron spatial resolution, which is a crucial condition for the spatial diagnostics of sharply focused short-wavelength VUV radiation and X-rays.**

Keywords: *laser ionisation of atoms and molecules, ion projection microscopy.*

1. Introduction

Field emission and field ion microscopy, which was invented by E.W. Müller and was the first to enable atomic-resolution imaging [1], is a rather effective tool for studying the surface of refractory metals [2]. The main components of a projection microscope (PM) that serves this purpose are a very sharp metallic tip of radius $r \sim 10$ nm and a position-sensitive detector, with a divergent accelerating electric field applied between them, which is very strong immediately near the tip. The principle behind the imaging of a portion of the tip surface is that charged particles resulting from field emission fly radially along the electric field lines from the tip to the detector. At sufficiently low r values, the projector principle ensures high image magnifications ($C \sim 10^4$ to 10^6). It is however of little utility in the case of many materials, including complex organic molecules, because the strong static electric field near the emitting surface distorts their structure (to the point of breakdown) [3].

The use of laser radiation in a PM allows one to avoid these adverse effects and obtain spectral information about the object of interest, as was first demonstrated by Letokhov [3]. In addition, he proposed that high spatial and temporal resolutions could be combined in a single experiment [4] through the use of ultrashort laser pulses in a PM. In contrast to what occurs in field emission microscopy, electrons (or ions) that produce an image can result from selective laser excitation followed by ionisation of a portion of a molecule with particular molecular bonding. The radial static electric field in a laser-driven PM serves only a 'transport' function. To simultaneously reach a nanometre spatial resolution and a pico- or femtosecond temporal resolution, the use of several ultrashort laser pulses with a particular time delay between them was proposed. Note that this method would allow one to follow the dynamics of a small group of molecules or even an individual molecule (in contrast to diffraction methods [5] that use ultrashort X-ray or electron pulses, which probe dynamics averaged over a relatively large ensemble of molecules).

The proposed scheme was used to demonstrate the possibility of photoion imaging at a magnification of ~1000$^\times$ while selectively exciting dye molecules [6]. However, the spatial resolution limit of the device, determined by the scatter (~10 eV) in the initial kinetic energy of molecular photoions desorbed from the surface, along with the destructive character of the method, severely limits its potential. Because of this, photoelectron projection microscopy is in many cases more attractive.

A hollow tip, e.g. a quartz nanocapillary tube, can be used instead of a classic tip. After producing a conductive organic polymer layer on such a capillary, an electrostatic potential can be applied to the tip apex, and the specimen can be examined by laser-assisted photoelectron projection microscopy [7]. In addition, a hollow tip allows one to produce spatially compressed electron bunches by passing photoelectron pulses through a nanocapillary tube [8]. The action of intense, sharply focused ultrashort laser pulses on moving electrons leads to photoelectron beam spreading due to the Gaponov–Miller force. Together with the projector principle, this allows one to combine spatial and temporal resolutions in a single experiment [9].

The ionic mode in a PM is of certain interest for the following application. The point is that projection microscopy is a sufficiently promising approach for studying the photoionisation of atoms and molecules (or clusters) in a strong laser field. As shown below, this does not even require to use a very sharp tip. The projection microscopy of photoionisation processes in gases considerably extends the application field of PMs.

Nonresonant ionisation of free atoms and molecules in a high-intensity laser field was the subject of a particular research direction in physics starting from a well-known theo-

S.A. Aseyev, B.N. Mironov, V.G. Minogin, A.P. Cherkun, S.V. Chekalin Institute of Spectroscopy, Russian Academy of Sciences, Fizicheskaya ul. 5, 142190 Troitsk, Moscow, Russia;
e-mail: chekalin@isan.troitsk.ru

Received 24 December 2012; revision received 24 January 2013
Kvantovaya Elektronika **43** (4) 308–312 (2013)
Translated by O.M. Tsarev

retical study by Keldysh [10]. The formalism proposed by him made it possible to adequately estimate the hydrogen atom ionisation probability as a function of laser radiation intensity [11] and to examine two photoionisation regimes: multiphoton and tunnelling (field-driven) processes. Later, this formalism was extended to more complex atomic and even molecular systems. One of the most impressive consequences of tunnelling photoionisation is probably the generation of attosecond pulses less than 10^{-15} s in duration in the spectral region between the VUV and soft X-rays [12].

To raise the intensity of attosecond electromagnetic bunches, these should be focused. Consequently, the resulting beams will, in the limit, have submicron transverse dimensions. The temporal characteristics of attosecond pulses can be measured using already existing techniques [12], but spatial diagnostics of such pulses currently presents serious difficulties. This is due in many respects to the fact that the resolution of short-wavelength detectors is limited by the size of an individual element (pixel) of the detector array, which is at best several microns. This generates interest in developing a different approach that would enable total spatiotemporal diagnostics of attosecond pulses.

The photoionisation probability depends both on laser radiation parameters and, in many respects, on the properties of the target itself (atoms, molecules or clusters), which has been the subject of extensive research [12]. Experimental studies of the photoionisation process in a strong laser field encounter a fundamental difficulty that a photoion signal is typically collected from the entire focal spot of a laser beam. Because of this, ions that arrive at the detector originate from regions differing in laser radiation intensity, which significantly impedes a direct comparison of experimental data and theoretical predictions. In this connection, it is important from the experimental point of view to develop a method that would enable a 'look inside' the focal spot of a high-intensity laser beam. Schultze et al. [13] have recently proposed one possible solution to this problem with the use of relatively high-technology equipment.

At the same time, as shown below there is an alternative way of visualising photoionisation processes in gases with a subdiffraction spatial resolution. It takes advantage of the projector principle and employs a metallic tip with a radius of curvature from tens to hundreds of microns. This approach is simpler than, e.g., the use of a time-of-flight reflectron with a 10-μm aperture [13] and does not require any 'scan' procedure, which would allow only part of information to be detected every time when a certain potential is applied to the electrostatic mirror of the reflector. This makes it possible to improve measurement accuracy and approach the problem of diagnosing single high-intensity laser pulses.

2. Experimental

Figure 1 shows a schematic of the experimental setup. Photoions are produced through the photoionisation of residual gas molecules in a vacuum system. The resulting ion bunch propagates in vacuum through a divergent electric field between a silver tip with a 0.5-mm radius of curvature and a flat detector. The signal is recorded using a position-sensitive scheme, which includes a pair of microchannel plates with an active region diameter of 25 mm and a phosphor screen. The image on the phosphor is recorded by a video camera and fed to a computer. The tip–detector distance L is 150 mm. An electric potential V_t = 10 kV is applied to the tip. The microscope is placed in a chamber, which can be pumped down to a vacuum of $\sim 10^{-7}$ mm Hg by a turbomolecular pump.

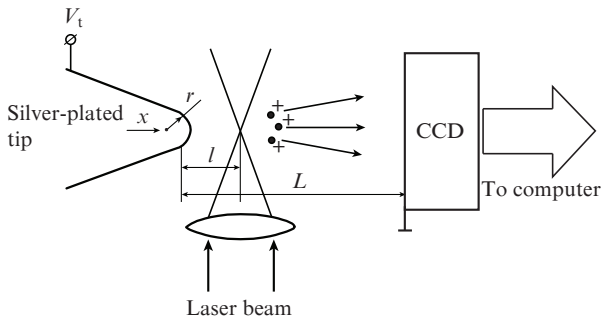

Figure 1. Schematic of the experimental setup.

In our experiments, we used 800-nm laser pulses with a duration $\tau \approx 40$ fs, repetition rate $f = 1$ kHz and energies of up to several hundred microjoules. The laser beam was focused by a lens with a focal length of 230 mm into vacuum a distance $l \approx 0.1$ mm from the tip. According to measurements performed in air with a standard laser beam profiler (the laser beam intensity was substantially lower than that in direct measurements under vacuum), the half-intensity beam waist diameter d was ~40 μm. When residual gas molecules in the chamber were ionised, the laser beam intensity in the centre of the focal waist, I_0, reached 3×10^{14} W cm^{-2}. According to time-of-flight mass spectrometry results, the predominant signal was that of H_2O^+. (The measurements were performed in the same vacuum chamber but with an electron multiplier tube instead of the position-sensitive detector.)

Recall that the magnification of a PM is given by the well-known formula [3]

$$C = L/(kr), \tag{1}$$

where the correction coefficient k takes into account the deviation of the geometry from sphericity, because a planar detection configuration was used instead of a poorly available spherical detector. To determine k and calibrate the microscope, a nickel gauze with an aperture size of 60 μm was applied to the tip. The procedure was performed with no adhesive. Next, the needle was placed in vacuum and a negative potential $V_t = -8$ kV was applied to it, which enabled photoelectron signal detection. To this end, the tip was exposed to a sharply focused 800-nm laser beam at an incident intensity of $\sim 10^{10}$ W cm^{-2}. Because of the difference in work function between silver and nickel, $W_{Ag} \approx 4.34.3$ eV and $W_{Ni} \approx 5$ eV [2], the photoelectron emission process was either three- or four-photon, respectively. The photoelectron image of the nickel gauze on the position-sensitive detector was darker, which allowed us to directly determine the correction coefficient for our geometry: $k \approx 2$. Under such conditions, the magnification C reached ~150×.

3. Experimental results and discussion

Figure 2 shows a photoion image on the position-sensitive detector and its x-axis profile. It is seen in Fig. 2b that the experimental profile is rather well represented by a Gaussian. The focused laser beam profile in our case can also be fitted by a Gaussian. For this reason, an approximation that uses a Gaussian distribution is natural in this study. This signifi-

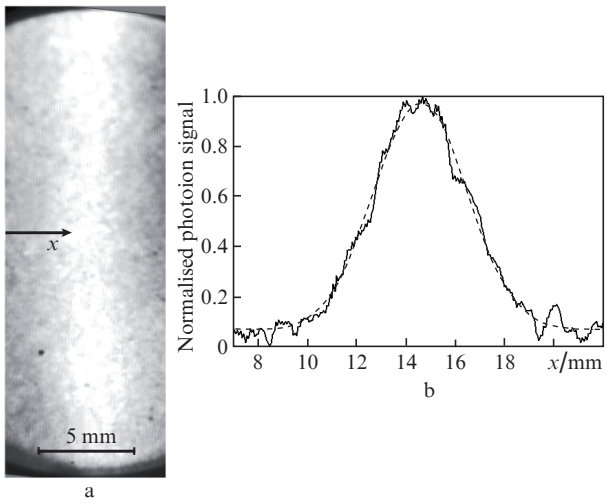

Figure 2. (a) Position-sensitive detector signal obtained through the photoionisation of water molecules in vacuum and (b) the x-axis profile of the signal. The dashed line represents the best fit to the experimental data with a Gaussian.

cantly simplifies analysis of the experimental data and allows us to perform calculations in analytical form.

The focal waist intensity is given by

$$I = I_0 \exp(-2r^2/w_0^2), \tag{2}$$

where $w_0 \approx 36$ μm is the beam radius under the conditions of this study. Recall that it was measured with a laser beam profiler. The confocal parameter, or depth of focus, $2\pi w_0^2/\lambda$, reaches ~9 mm, which is about one order of magnitude greater than the tip diameter.

The water molecule photoionisation probability is approximately

$$P \propto I^n, \tag{3}$$

where $n \approx -2/[3\sqrt{I_{au}} \ln I_{au}] - 0.25$. The dimensionless parameter I_{au} is given by $I_{au} \approx I/3.5 \times 10^{16}$ W cm^{-2}. We take into account that the tunnelling photoionisation rate is [14]

$$P_{tun} \sim \exp[-0.67/\sqrt{I_{au}}]/I_{au}^{1/4}. \tag{4}$$

Neglecting the Coulomb repulsion (under the present experimental conditions, the focal waist contained only about 100 molecules), we find that the width of the Gaussian distribution observed on the detector was

$$w_{obs} \approx C^* w_0 / \sqrt{n}, \tag{5}$$

where $C^* = L/[k(r + l)] \approx 125$.

One important point warrants mention here. In experiments, a three-dimensional (3D) image is projected onto a flat screen. For analysis, the entire volume can be divided into individual layers, with the plane of each layer normal to the plane of the detector. Projecting a layer, i.e. the two-dimensional $f(r)$ distribution, possessing a centre of symmetry, onto, e.g., the y axis in the plane of the detector, we obtain a dependence of the form $\int f(\sqrt{x^2 + y^2})dx$, which in general does not reproduce the input function $f(r)$. An important exception is the Gaussian distribution. Otherwise, to reproduce $f(r)$ one has to deconvolve a planar image and, e.g., use an Abel inversion-based algorithm, like in analysis of the initial velocity distribution of electrons photoemitted from atomic and molecular targets (velocity map imaging [15]).

As mentioned above, the use of the Gaussian distribution allows one to simplify analysis. In particular, we obtain directly from (5) $w_0 \approx 35 \pm 5$ μm, in good agreement with laser beam profiling data. The estimated error $\Delta w_0 \approx 5$ μm arises from the uncertainty in least-squares fitting the measured profile in Fig. 2b by a Gaussian.

The spatial resolution in our method is limited by the initial-velocity component normal to the accelerating electric field. An ion having a nonzero initial energy, δK, will be detected by the detector with a spatial uncertainty

$$\delta \approx L\sqrt{\delta K/(eV_t)}. \tag{6}$$

This leads to the following measurement uncertainty:

$$\Delta_{obs} \approx \delta/C \approx kr\sqrt{\delta K/(eV_t)}. \tag{7}$$

Taking $k = 2$, $r = 0.5$ mm, $\delta K \approx 30$ meV and $eV_t = 10$ keV and neglecting the Coulomb repulsion in the photoion bunch, we find that the scatter in energy at room temperature leads to $\Delta_{obs} \approx 1.6$ μm, which is of the same order as Δw_0. Recall that δK and, hence, Δ_{obs} can be reduced by performing measurements in a cooled pulsed gas jet.

The spatial resolution can be drastically improved by using a sharper tip. It follows from relation (7) that, at a tip radius $r \approx 30$ μm, the spatial resolution is $\Delta_{obs} \approx 0.1$ μm. It is worth pointing out that direct experimental determination of the correction coefficient k in (1) for such a microtip may present a serious problem: the magnification for a sharp tip with 30 μm reaches 2500×.

4. Applications of the method

In this section, we consider two possible applications of the method under development. One of them is measurements of the X-ray pulse profile at the output of a dielectric microcapillary tube. Note that an X-ray microsource can be manipulated using a vacuum microscope created in our laboratory (Fig. 3). It is intended for studies of nanoscale laser desorption of molecular complexes and has two interesting potential capabilities. Firstly, the flat surface with a specimen is exposed to laser pulses, and the forming molecular ions are directed through a microcapillary tube to the detector of a time-of-flight spectrometer (Fig. 4). In the visible range, however, the size of the laser-exposed zone considerably exceeds the aperture of the capillary tube, d_a, which may be 100 nm or less in commercially available hollow silica tips [16]. Therefore, to avoid information losses the electromagnetic field immediately below the tip should be intensified.

In another geometry, an X-ray pulse can be passed through a capillary tube, thus ensuring both high spatial resolution and complete information acquisition. In an earlier experimental study, we demonstrated the possibility of molecular complex desorption by soft X-rays resulting from the exposure of a solid target to a single sharply focused femtosecond laser pulse with an energy of ~1 mJ. This allows one to study surfaces with high spatial resolution in combination with high elemental (chemical) selectivity and observe the photodesorption process in real time [17].

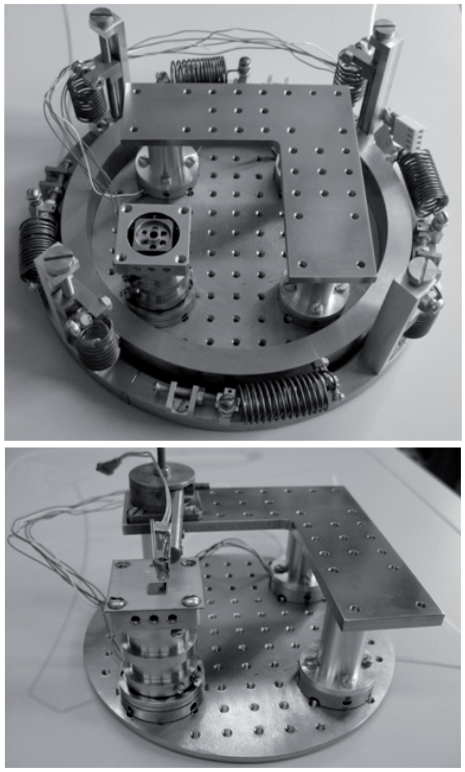

Figure 3. Vacuum scanning probe microscope with a hollow tip: photographs of the microscope (a) with no capillary tube and (b) with a capillary tube but without the spring suspension.

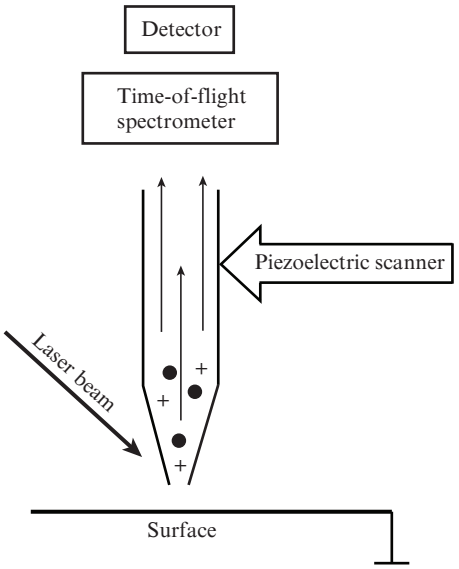

Figure 4. Schematic of nanoscale photodesorption of molecular ions.

The question of spatial resolution remains, however, open. The point is that soft X-rays can pass through the thin wall at the capillary tube tip. Because of this, the X-ray beam diameter may differ from the microaperture size. The cross-sectional area of an X-ray bunch can be measured using the approach described in this paper.

In the future, the use of a vacuum scanning probe microscope will allow one to observe photoemission processes on a planar surface with a subdiffraction (down to 10 nm) spatial resolution. To this end, photoelectrons resulting from laser irradiation of a sample will be passed through a capillary tube. We note once more that, according to Grams et al. [16], the aperture diameter at the end of a hollow dielectric tip can be reduced to 10 nm.

Secondly, our method can be used for spatial diagnostics of laser radiation in a broad spectral range. Basically, this range is determined by the spectral transmission of the window between the air and vacuum. One possible beam profiler configuration is shown schematically in Fig. 5. The profiler has the form of an evacuated quartz envelope, which houses a photocathode (thin metallic layer grown by evaporation on a tip with a radius of curvature in the range $\sim$0.1–0.5 mm) and a detector (phosphor with a thin conductive layer grown by evaporation). Special-purpose slits can be made on the cathode surface for profiler calibration. For operation of the device, a high voltage of about 10 kV should be applied between the electrical leads of the photocathode and phosphor screen. Information from the detector can be fed to a computer using a standard recording scheme with a sensitive CCD video camera. One important advantage of this device is the possibility of directly diagnosing the focal region of sharply focused, micron-size laser beams without any additional optics for changing laser beam dimensions.

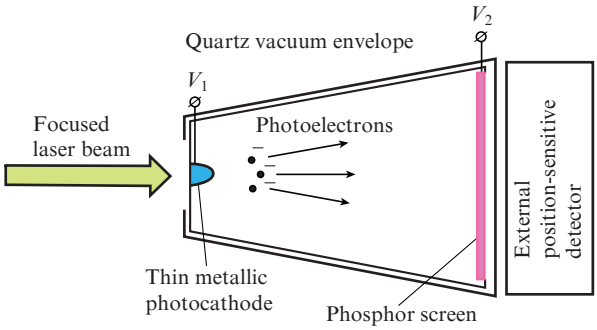

Figure 5. Schematic of a broadband laser beam profiler. (Note that laser radiation can in principle be introduced through the lateral surface of the envelope.)

5. Conclusions

We have proposed and experimentally tested a method for investigating photoionisation processes in atoms, molecules and small clusters with a high, subdiffraction spatial resolution. The present results demonstrate that the use of a metallic needle with a submillimetre-size tip and a standard position-sensitive ion recording scheme enables direct visualisation of sharply focused laser radiation at a magnification of $\sim$100×. The resolution of the method is not limited by the size of an individual element (pixel) of the detector intended for beam profile imaging or by the spectral range of conventional CCD arrays. According to our estimates, spatial nanodiagnostics of a sharply focused attosecond pulse requires a tip radius of $\sim$10 μm. Magnification will then reach several hundred.

Acknowledgements. This work was supported in part by the Presidium of the Russian Academy of Sciences (Extreme Light Fields and Their Applications Programme) and the

Russian Foundation for Basic Research (Grant Nos 11-02-00796 and 10-02-00469).

References

1. Muller E.W. *Z. Phys.*, **131**, 136 (1951).
2. Oura K., Lifshits V.G., Saranin A.A., Zotov A.V., Katayama M. *Surface Science – An Introduction* (Berlin: Springer-Verlag, 2003).
3. Letokhov V.S. *Phys. Lett. A*, **51**, 231 (1975).
4. Letokhov V.S. *Laser Control of Atoms and Molecules* (Oxford: Oxford University Press, 2007).
5. Srinivasan R., Feenstra J.S., Park S.T., Xu S., Zewail A.H. *Science*, **307**, 558 (2005).
6. Chekalin S.V., Letokhov V.S., Likhachev V.S., Movshev V.G. *Appl. Phys. B*, **33**, 57 (1984).
7. Mironov B.N., Aseev S.A., Chekalin S.V., Ivanov V.F., Gribkova O.L. *Pis'ma Zh. Eksp. Teor. Fiz*., **92** (11), 860 (2010).
8. Aseyev S.A., Mironov B.N., Chekalin S.V., Letokhov V.S. *Appl. Phys. Lett*., **89**, 112513 (2006).
9. Aseev S.A., Mironov B.N., Minogin V.G., Chekalin S.V., Letokhov V.S. *Pis'ma Zh. Eksp. Teor. Fiz*., **90** (1), 15 (2009).
10. Keldysh L.V. *Zh. Eksp. Teor. Fiz*., **47** (5), 1946 (1964).
11. Bohan A., Piraux B., Ponce L., Taïeb R., Veniard V., Maquet A. *Phys. Rev. Lett*., **89**, 113002 (2002).
12. Krausz F., Ivanov M. *Rev. Mod. Phys*., **81**, 163 (2009).
13. Schultze M., Bergues B., Schröder H., Krausz F., Kompa K.L. *New J. Phys*., **13**, 033001 (2011).
14. Tong X.M., Zhao Z.X., Lin C.D. *Phys. Rev. A*, **66**, 033402 (2002).
15. Eppink A.T.J.B., Parker D.H. *Rev. Sci. Instrum*., **68**, 3477 (1997).
16. Grams M.P., Cook A.M., Turner J.H., Doak R.B. *J. Phys. D: Appl. Phys*., **39**, 930 (2006).
17. Mironov B.N., Aseev S.A., Chekalin S.V., Ivanov V.F., Gribkova O.L. *Pis'ma Zh. Eksp. Teor. Fiz*., **96**, 670 (2012).